Evaluating the Ability of External Electric Fields to Accelerate Reactions in Solution

Miriam Aziz[1†], Claudia R. Prindle[1†], Woojung Lee[1], Boyuan Zhang[2], Cedric Schaack[3], Michael L. Steigerwald[1], Fereshteh Zandkarimi[1,4], Colin Nuckolls[1]*, and Latha Venkataraman[1,5]*

[1]Department of Chemistry, Columbia University, New York, New York 10027, United States

[2]Department of Chemistry, Fairfield University, Fairfield, Connecticut 06824, United States

[3]Department of Chemistry, Wake Forest University, Winston-Salem, North Carolina 27109, United States

[4]Mass Spectrometry Core Facility, Department of Chemistry, Columbia University, New York, New York 10027, United States

[5]Department of Applied Physics and Applied Mathematics, Columbia University, New York, New York 10027, United States

[†]equal contribution

Corresponding authors: Email: cn37@columbia.edu; lv2117@columbia.edu

ABSTRACT

This study investigates the catalytic effects of external electric fields (EEFs) on two reactions in solution: the Menshutkin reaction and the Chapman rearrangement. Utilizing a scanning tunneling microscope-based break-junction setup and monitoring reaction rates through high-performance liquid chromatography connected to a UV detector (HPLC-UV) and an ultraperformance liquid chromatography coupled with quadrupole time-of-flight mass spectrometry (UPLC-q-ToF-MS), we observed no rate enhancement for either reaction under ambient conditions. Density functional theory (DFT) calculations indicate that electric-field-induced changes to reactant orientation and the minimization of activation energy are crucial factors in determining the efficacy of EEF-driven catalysis. Our findings suggest that the current experimental setups and field strengths are insufficient to catalyze these reactions, underscoring the importance of these criteria in assessing reaction candidates.

INTRODUCTION

The field of green chemistry has garnered widespread interest in recent decades, due to its ability to harness chemical innovation to meet environmental and economic goals that benefit research, industry, academia, and the environment[1]. Out of all the subfields of green chemistry, advances in catalysis stand out as especially promising[2-7]. In particular, novel heterogeneous catalysis methods have led to increased reaction efficiency, enhanced product selectivity, reduced purification costs, and minimized chemical waste[8,9]. Yet, catalyst availability, cost, and longevity remain obstacles. Thus, researchers wishing to solve these challenges have started shifting their focus toward a novel class of non-reagent-based catalysts: external electric fields (EEFs)[10].

While there have been many computational investigations into EEFs as potential heterogeneous catalysts[11-15], only a few experimental studies have demonstrated the catalytic effect of EEFs[16-22]. For example, Aragonès et al. showed that the rate of a Diels-Alder reaction could be enhanced using an oriented EEF[23]. In this study, a diene molecule was covalently attached to a Au scanning tunneling microscope (STM) tip and positioned above a monolayer of dienophile molecules bound to the Au STM substrate. The oriented electric field between the STM tip and substrate was along the reaction axis and catalyzed the Diels-Alder cycloaddition. The product was detected using *in-situ* conductance measurements. Although this study was the first to report experimental evidence supporting the catalytic effect of EEFs, the reaction was at the single-molecule scale and was not characterized by standard techniques such as NMR, high-performance liquid chromatography (HPLC) with a UV detector or mass spectrometry (MS). A related Diels-Alder reaction was studied by Huang et al. where they showed a 10-fold rate enhancement of the rearomatization of the Diels-Alder product driven by an EEF[24]. While these findings highlight a new reaction that is catalyzed by electric fields, these fields also require fixed orientation along

the reaction axis. For solution-based EEF-driven chemistry, this would require the reactants to have sufficiently large intrinsic dipole moments along the preferred reaction axis to self-align in the external field, making large-scale electric-field-driven catalysis challenging.

Recent studies from our groups have attempted to address such limitations of preorientation. For example, Zang et al. demonstrated the ability of electric fields to catalyze the isomerization of a *cis*-[3]cumulene to a *trans*-[3]cumulene through the application of an electric field via an STM-based break-junction setup (STM-BJ)[25]. While previous studies required the preorientation of molecules to a surface or fixed oriented electric fields, Zang et al. observe catalysis of the *cis*-to-*trans* isomerization in solution. More recently, Zhang et al. showed that electric fields can drive the bond homolysis of an oxygen-oxygen bond in 4-(methylthio)benzoic peroxyanhydride at ambient temperatures in bulk solution, without the use of co-initiators, light, or chemical activators[26]. Notably, these studies were also the first reported use of electric-field-driven catalysis determining rate enhancement using *ex-situ* characterization techniques, such as HPLC with UV detection, highlighting potential applications of these results on larger reaction scales.

Despite experimental evidence of reactions being catalyzed by electric fields, there are few clear guiding principles for determining which reactions may be viable candidates for electric-field-driven catalysis. In particular, Shaik et al. have highlighted the importance of alignment between the applied electric field and the reaction axis[10]. Through computational investigations, they have shown that the more a field is aligned with (or parallel to) the reaction axis, the greater the predicted catalytic effect of the field.[27] Conversely, depending on the reaction, a field antiparallel to the reaction axis can have an inhibitory effect on catalysis[28]. Additionally, if multiple reaction axes lead to different products, then alignment of the field with one reaction axis

versus the other can determine chemo- or regioselectivity[29-31]. Furthermore, a theoretical investigation by Hoffmann et al. illustrated the importance of reaction dipoles in electric-field-driven catalysis[32]. They establish a linear free energy relationship (LFER) between the change in activation energy ($\Delta\Delta G^{\ddagger}$) and the change in reaction energy ($\Delta\Delta G_{rxn}$) that are related by a constant of proportionality $m = \frac{\Delta\mu^{\ddagger}}{\Delta\mu_{rxn}}$ (where $\Delta\mu^{\ddagger} = \mu_{TS} - \mu_R$ is the change in dipoles between transition state and reactant, and $\Delta\mu_{rxn} = \mu_P - \mu_R$ is the change in dipoles between product and reactant) and both the sign and magnitude of this constant determine the sensitivity of the activation energy to changes in the reaction energy. Therefore, assessing the changes in dipoles throughout a reaction can determine how an electric field – in stabilizing certain reaction species dipoles – affects the kinetics and thermodynamics of a chemical reaction. However, most of these computational theories have yet to be experimentally substantiated.

Here, we study two different reactions in solution that have been theorized to undergo electric-field-driven catalysis – the Menshutkin reaction, and the Chapman rearrangement – to help narrow the criteria for selecting and studying electric-field-driven reactions. We test the effect of external electric fields using an STM-BJ setup and monitor reaction rates *ex situ* using liquid chromatography methods. We apply voltage biases in the STM-BJ to generate electric fields *in situ*, and observe no rate enhancement for either reaction at ambient conditions, despite following previously successful protocols[25,26]. Using density functional theory (DFT) calculations, we hypothesize that reactant orientation and activation energy are critical for determining whether a reaction can be accelerated in an electric field. From these results, we help outline a new set of guidelines for studying reactions in electric fields.

METHODS

STM-BJ

Conductance measurements were performed using a custom-built scanning tunneling microscope[33]. The electric field is applied between a 0.25 mm gold wire (99.998%, Alfa Aesar) and a gold-coated (99.999%, Alfa Aesar) steel puck (Ted Pella) as the gold substrate. We prepare molecular solutions at varying concentrations in either propylene carbonate (PC) or tetradecane (TD), purchased from Thermo Fisher Scientific and used without further purification. For measurements performed using PC, Au tips are prepared by driving a mechanically-cut tip through Apiezon wax to suppress background capacitive current[34]. The Au tip is brought in and out of contact with the Au substrate while the current (I) through the junction is continuously measured at an applied voltage (V) to determine the conductance by $G = I/V$. A 100 kΩ series resistor is used in the circuit to avoid saturating the current amplifier. A conductance plateau below $1G_0 = 2e^2/h$ is observed as a molecule bridges the gap between the electrodes to form a single-molecule junction. We repeat this process and collect >5000 conductance versus displacement traces, which we analyze to get statistically-relevant information. Data collection and analysis are collected with custom software written in Igor Pro (Wavemetrics).

For the Menshutkin reaction, a 100 mV bias was applied to solutions of 150 mM benzyl bromide and 1.5 mM 4-phenylpyridine in either PC or TD to generate an electric field between a Au tip and substrate. Conductance measurements were not compiled due to lack of aurophilic binding groups in our reaction system. For the Chapman rearrangement, both 100 mV and 750 mV biases were applied to 1 mM solutions of the reactants and products in TD, and conductance measurements were compiled.

Calculations

DFT calculations were performed with the FHI-AIMS package[35-37]. We first relax the geometry of the reactant and product of the Menshutkin and Chapman reactions using the Perdew-

Burke-Ernzerhof (PBE) functional and a "light" basis set (equivalent to a single-zeta basis).[38] We use standard convergence criteria and ensure that forces on all atoms were under 10^{-2} eV $Å^{-1}$. Note that calculations that use DFT have errors inherent to the method. We measure the length between the C and N that forms a bond in the reactions. We then modify the coordinates of the relaxed geometry of the reactants to align specific atoms—the C and N that form a bond—along the z-axis. We then decrease the C-N distance in steps of 0.1 Å and relax the reactants while constraining the C-N distance, concluding this process once the C-N distance is less than the measured reactant bond length by approximately 0.3 Å. For the Menshutkin reaction, we additionally constrain the Br atom to be on the same axis as the C and N that form a bond. Without this constraint, the lowest energy geometry has considerable overlap between the two pi-systems. We plot the total energy as a function of C-N distance. We next calculate the dipole moments of each relaxed geometry at all C-N distances. To calculate the energy change caused by applying the electric field, we use $\Delta E = -\vec{\mu} \cdot \vec{E}$, where $\vec{\mu}$ is the calculated dipole moment, and $\vec{E}$ is 0.1 V/Å or 0.25 V/Å. We convert this product to eV. To find the energy of each geometry in the field, we subtract this change from the energy of the relaxed molecules with no field applied at each C-N distance. Finally, we plot the total energy with the field as a function of C-N distance. Note that this calculation is quite accurate and comparable to a full calculation including an explicit electric field as shown in SI Figure 2b.

To determine the energy of the reactant and product embedded in water, we use Jaguar.[39] We relax both the reactant and product with and without water (using an implicit solvent model) and determine the energy difference due to the presence of water. Note that the dielectric constant of PC is 64 while that of water is around 80.

Liquid Chromatography and Mass Spectrometry

HPLC–UV analysis was carried out on an Agilent LC1220 HPLC instrument with diode array detector using Agilent Zobrax Eclipse Plus C18 column (5 μm x 21.2 mm x 250 mm). The column was maintained at 25°C. For Menshutkin experiments, the mobile phase was water: acetonitrile containing 10 mM ammonium acetate buffer (50:50; v/v), with a flow rate of 1 mL/min. Peaks corresponding to compounds **2** and **3** are integrated at a detection wavelength of 280 nm. Calibration plots relating integration area and concentration are generated by running concentrations of **2** and **3** in triplicate, integrating the area under each peak, making a plot of concentration (μM) versus integration, and fitting a line to these points. Each calibration plot has a coefficient of determination greater than 0.99 ($R^2 \geq 0.99$). For Chapman experiments, the mobile phase was water:acetonitrile (30:70; v/v) , with a flow rate of 1 mL/min. Peaks corresponding to compounds **4** and **5** are integrated at a detection wavelength of 260 nm and 270 nm, respectively. Peaks are integrated using Agilent LC1220 HPLC automated software.

For ultraperformance liquid chromatography coupled with quadrupole time-of-flight mass spectrometry (UPLC-q-ToF-MS), the extracted samples were separated using an ACQUITY UPLC BEH C18 (2.1 mm x 50 mm x 1.7 μm) on an Aquity UPLC H-Class chromatography system. Mobile phase A consisted of water and mobile phase B was acetonitrile, both containing 0.1% formic acid. After the injection, the gradient was held at 20% mobile phase B for 0.5 min and increased to 99% B in 7 min and stayed at 99% B for 1.5 min. The eluent composition returned to the original condition in 0.5 min, and the column was re-equilibrated for an additional 1 min before the next injection was conducted. The oven temperature was set at 35 ˚C, and the flow rate was 450 μL min^{-1}. The injection volume was 2 μL using the flow-through needle mode. The Xevo G2-XS-Q-ToF mass spectrometer was operated in positive electrospray ionization mode. A capillary voltage and sampling cone voltage of 1.8 kV and 30 V were used, respectively. The

source and desolvation temperatures were kept at 120 ˚C and 450 ˚C, respectively. Nitrogen was used as the desolvation gas with a flow rate of 700 L hr^{-1}. The data were collected in duplicates over the mass range *m/z*: 50 to 1,200 Da. The low collision energy was set to 4 eV, and the trap collision energy was ramped from 15-40 eV. The data were acquired with MassLynx (version 4.2) software.

RESULTS & DISCUSSION

Menshutkin Reaction

We first explore the electric-field-driven catalysis of the Menshutkin reaction, which is an S_N2 reaction between a tertiary amine and an alkyl halide that forms a quaternary ammonium salt (**Figure 1a**). This reaction has been theorized to be catalyzed by an electric field.[27,28] We chose reactants (benzyl bromide **1**, 4-phenylpyridine **2**) and products (4-phenylpyridinium salt **3**) with aryl groups **(Figure 1b**) so that reaction kinetics could be assessed *ex situ* using HPLC with UV-visible detection (**Figure 1c, top**). Additionally, since the STM-BJ operates under ambient conditions, **1**, **2**, and **3** were selected due to their low vapor pressure, in order to avoid changes in their concentrations due to evaporation over the time scale of the measurements.

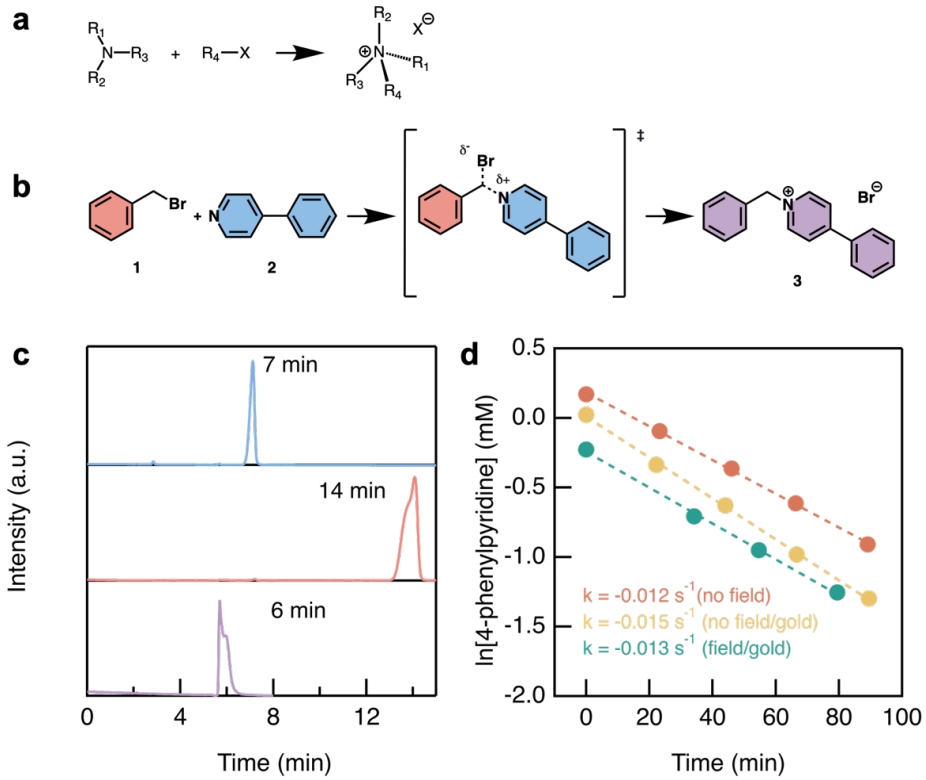

Figure 1. (a) General Menshutkin reaction scheme. (b) Menshutkin reaction scheme containing benzyl bromide (red, **1**), 4-phenylpyridine (blue, **2**), and the salt product (purple, **3**). (c) HPLC chromatograms of **1**, **2**, and **3**. (d) Pseudo first-order kinetic plots of the Menshutkin reaction with no field applied under ambient conditions (orange), with no field applied on a Au-coated steel puck (yellow), and with a field applied on a Au-coated steel puck (green) in propylene carbonate (PC).

To determine the catalytic effect of electric fields on the Menshutkin reaction, we prepare reaction mixtures of 150 mM **1** and 1.5 mM **2** in both a polar solvent (propylene carbonate, PC, dielectric constant ε=65) and a nonpolar solvent (tetradecane, TD, dielectric constant ε=2). While we generally use non-polar solvents when testing electric field-driven reactivity, we also use a polar solvent in our studies of the Menshutkin reaction, as it is well established that this reaction is accelerated in polar solvents[40,41]. The reaction was run in three environments: in a vial under ambient conditions, on a Au-coated STM substrate under ambient conditions, and on a Au-coated

STM substrate with the solution exposed to an electric field following the protocol developed from previous experiments.[25,26] An electric field was created by applying a bias of 100 mV between the electrodes in the STM-BJ setup (see Methods). The reactions that were run in a vial and on a Au-coated STM substrate were control measurements to account for reactivity occurring under ambient conditions or in the presence of Au. To monitor the reaction progress in PC, we prepared solutions with known concentrations of **1**, **2**, and the product **3** and separated each in triplicate using HPLC with UV-visible detection (**Figure 1c**). Calibration curves were created to quantify the concentration of reaction species throughout an experiment (see Supporting Information for details). For each experiment, we took 20 μL aliquots every 20 minutes for approximately 90 minutes to compare the reaction kinetics both in and out of an electric field.

We applied a pseudo first-order rate law to determine the rate constant of each reaction condition: under no field (ambient conditions in solution), under no field on gold (ambient conditions on Au-coated steel puck) and under a field (on Au-coated steel puck in the STM-BJ setup) in PC. We confirm that the reaction obeys first-order kinetics, observing a linear relationship between the natural log of the concentration of **2** and time (**Figure 1d**). The rate constant k, represented by the slope, for each reaction condition is approximately the same (ranging from 0.012 to 0.015 s^{-1}), regardless of the presence of the electric field. Similar results are obtained for the Menshutkin reaction run in TD, where the reaction did not proceed for each reaction condition (**Figure S2**). This suggests that the electric field does not accelerate the Menshutkin reaction within experimentally accessible fields.

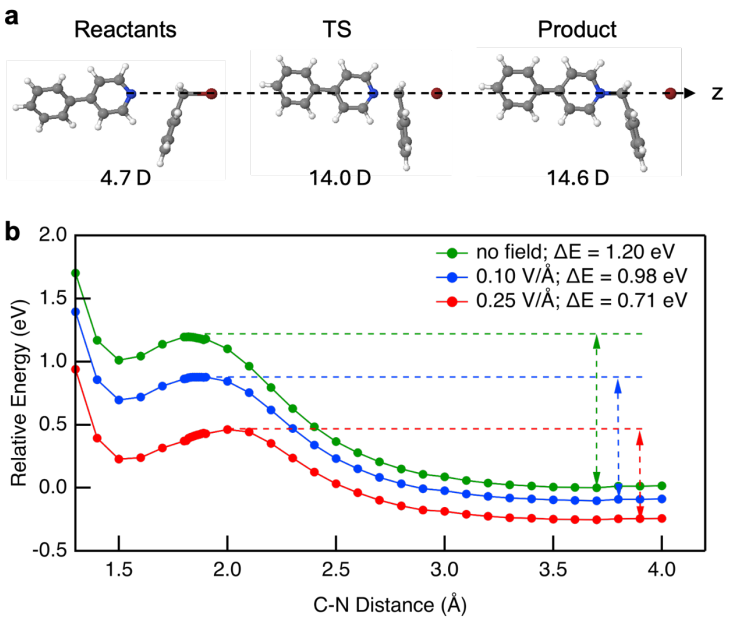

Figure 2. (a) DFT-optimized geometries of the Menshutkin species throughout the reaction. C, N, and Br atoms are constrained along the z-axis (dotted line), labeled with their respective dipole moments. (b) DFT-calculated energies of reaction species with different C-N bond distances, without field (green), with 0.1 V/Å electric field (blue) and 0.25 V/Å electric field (red). Energy barriers are indicated in the figure legend.

Under ambient conditions, the Menshutkin reaction proceeds through an S_N2 mechanism, where a bond is formed between the nitrogen of a tertiary amine and the carbon alpha to a halide to generate a quaternary ammonium salt, and the alkyl-halide bond is simultaneously cleaved[42,43]. To better understand the reaction and our results, we performed DFT calculations using the FHI-AIMS package[35-37]. We first relax the geometry of the reactants constraining the pyridyl N, benzylic C and Br on the z-axis as detailed in the Methods section.[38] We next decrease the C-N distance in steps of 0.1 Å and relax the reactants with the additional constraint that fixes the C-N distance (**Figure 2a**). This allows us to obtain the total energy and system dipole moment as a function of the C-N distance (**Figure 2b**, green curve). We obtain an energy maximum at a C-N distance of 1.8 Å and a new local minimum at a distance of 1.5 Å. We next calculate the dipole

moments of the reactant, transition state and product to test whether this reaction would indeed show an acceleration based on the LFER[32]. Using the values from our calculation, we obtain a proportionality constant relating $\Delta G^{\ddagger}$ and ΔG_{rxn}, m = +1.07. Therefore, if this LFER holds for electrostatic catalysis, an electric field should stabilize both transition state and product of the Menshutkin reaction relative to reactants. This suggests that an electric field should lower both the activation energy $\Delta G^{\ddagger}$ and the reaction energy ΔG_{rxn}, resulting in a reaction that is more thermodynamically and kinetically favorable in an electric field.

To illustrate the effect of the field, we calculate the change in energy of the reactants and products at each C-N distance in an experimentally accessible field of 0.1 V/Å. We do so by evaluating the energy change $\Delta E = -\vec{\mu} \cdot \vec{E}$, where $\vec{\mu}$ is the dipole moment calculated from outside of an electric field, and $\vec{E}$ is the applied field strength. We then plot the energies of the reactant species at different C-N bond distances when an electric field of $\vec{E}$ = 0.1 V/Å is applied (**Figure 2b**, blue curve) and compare them to the same energies without an electric field. Although the field lowers the energy of both the transition state and product, the changes are not significant since the calculated activation barrier in the field (0.98 eV) evidently remains too large for the field to overcome. We further determined how the energy difference between the product and reactant would be altered by a solvent with a large dielectric, as the product is zwitterionic. We find that the product is stabilized by ~1 eV relative to the reactant when using an embedded implicit solvent model with water (see Methods).

To rationalize our findings, we first note that the fact that the reaction proceeds without a field in PC (although not in TD) and is not accelerated in a field in either TD or PC is consistent with the calculated results. We find that the activation energy of the reaction is likely too large in nonpolar solvents, even in modest experimentally accessible fields. It is also well known that under

ambient conditions, the Menshutkin reaction proceeds at faster rates in more polar solvents, in part due to increased solvation of the polar transition state and product[41,44]. In PC, our experiments indicate that the change in reaction rate with and without an electric field is not significant enough to be observed, which is consistent with the small change in the transition state energy due to an electric field as seen in our calculations. Additionally, since the volume of solution exposed to the field in the STM-BJ setup is small, a much larger field might be needed to see any noticeable rate difference. Furthermore, as has been previously shown[28], alignment of the reaction axis with the electric field is critical in determining the potential degree of rate enhancement. Depending on how the reactants orient themselves in an external electric field, the reaction axis may not be perfectly aligned with the electric field vector, leading to changes in activation energies.

Chapman Rearrangement

To avoid the potential limitations of bimolecular reactions orienting unpredictably in an electric field, we chose to next investigate the electric-field-driven catalysis of an intramolecular reaction – the Chapman rearrangement – using the STM-BJ setup. The Chapman rearrangement is an intramolecular reaction that thermally converts *N*-arylbenzimidates to *N*-aroyldiphenylamines via a dipolar transition state, and typically requires very high temperatures (>250˚C) (**Figure 3a**). To assess the electric-field-driven catalysis of this reaction, we designed substrate systems compatible with STM-BJ measurements. We designed and synthesized a benzimidate reactant (**6**) and amide product (**7**) with thioanisole linkers to enable binding in the STM-BJ and *in-situ* monitoring of reaction kinetics (**Figure 3b**). We installed a nitro group *in the 2-position of the aroyl moiety* to provide a reaction with a lower activation energy[45,46]. The reaction rates were also quantified *ex situ* using HPLC-UV and UPLC-MS. We focus here on the transformation of nitro-

substituted *N*-arylbenzimidate to nitro-substituted *N*-aroyldiphenylamine (**6** → **7**). Details of the results for the substrates without nitro groups (**4** → **5**) are in the Supporting Information.

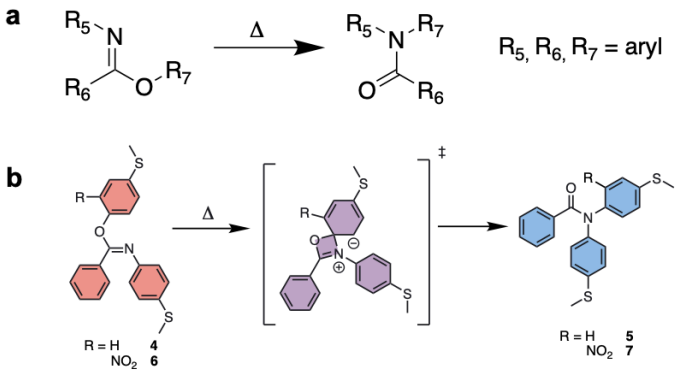

Figure 3. (a) General reaction scheme of the Chapman rearrangement. (b) Chapman rearrangement converting *N*-arylbenzimidates (**4** and **6**) to *N*-aroyldiphenylamines (**5** and **7**). Substrates are either with or without a nitro group.

To determine the catalytic effect of electric fields on the Chapman rearrangement, we both apply an electric field and take molecular conductance measurements using an STM-BJ setup to monitor reaction progress *in situ* (see Methods). First, we prepare 1 mM solutions of **6** and **7** in tetradecane (TD) and obtain one-dimensional (1D) histograms of each at an applied bias of 100 mV (**Figure 4a**). We observe molecular conductance peaks at approximately $3.7 \times 10^{-5} G_0$ and $1.5 \times 10^{-4} G_0$, confirming the formation of single-molecule junctions of **6** and **7**, respectively. This conductance difference is significant, allowing us to monitor reaction progress *in situ* by evaluating the evolution of single-molecule conductance over time. We then test whether an electric field has a catalytic effect on the Chapman rearrangement by depositing a 1 mM solution of **6** in TD on a Au substrate and applying a 750 mV bias in the STM-BJ for 48 hours. A comparison of histograms of the first and last 5,000 single-molecule conductance traces shows no difference, indicating that we measured the same molecular species (**6**) before and after the field is applied.

We also monitor the reaction *ex situ* using UPLC-MS to determine whether the reaction rate is accelerated in a field. We determine that **6** and **7** have different retention times of 4.6 and 4.1 minutes, respectively (see Methods), enabling us to detect these molecular species in our reaction mixtures (**Figure 4c**, top and bottom panels). After applying an electric field with a 750 mV bias in the STM-BJ, we take an aliquot of the reaction solution and analyze the samples on the UPLC-MS, observing a peak corresponding to the starting material **6**, but no peak corresponding to product **7**. These results suggest that there is no rate acceleration of the Chapman rearrangement in the electric field.

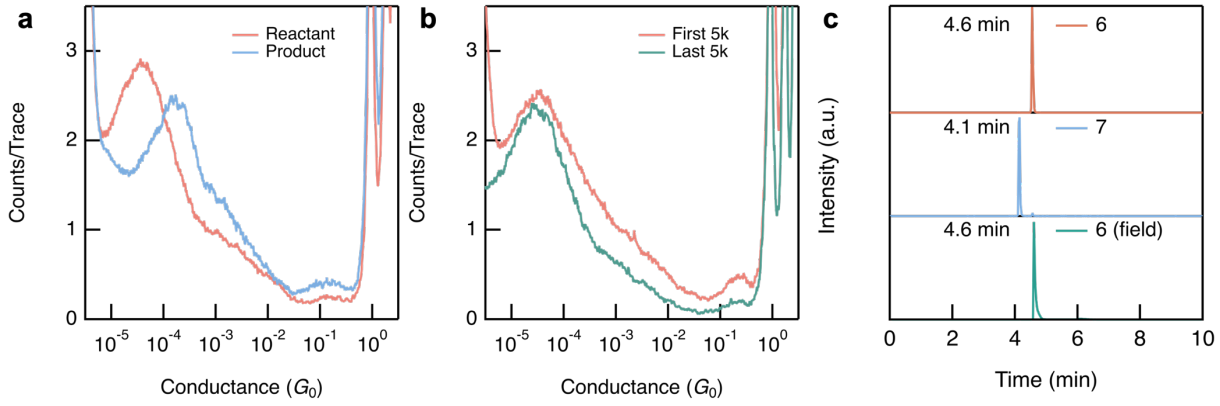

Figure 4. Logarithmically binned 1D histograms of (a) **6** and **7** (red and blue, respectively) and (b) **6** measured in TD before (red, first 5,000 traces) and after (green, last 5,000 traces) applying a 750 mV bias for 48 hours. (c) UPLC-MS chromatograms of **6**, **7**, and **6** after exposure to an electric field in the STM-BJ setup for 48 hours.

To better understand our findings, we again performed DFT calculations as detailed in the Methods section, and constrain the imidate nitrogen and the *ipso* carbon along the reaction axis We again decrease the C-N distance in steps of 0.1 Å and relax the reactants constraining the C-N distance. This allows us to obtain the total energy and system dipole moment as a function of the C-N distance. We obtain an energy maximum at a C-N distance of 1.9 and 2.0 Å (for **4** and **6**,

respectively) and a new local minimum at 1.4 Å (for both). Using dipole moment values calculated of the reactants, transition states, and products, we obtain m = 1.02 and 2.03, with and without the nitro groups, respectively. We again calculate the change in energy of the reactants and products at each C-N distance in a field of 0.1 V/Å and 0.25V/Å to illustrate the effect of the field ($\Delta E = -\vec{\mu} \cdot \vec{E}$). We observe that the activation barrier is decreased by only modestly with and without the nitro group. Thus, it is likely that the activation energy barrier of the Chapman rearrangement is too large to overcome in experimentally accessible electric fields.

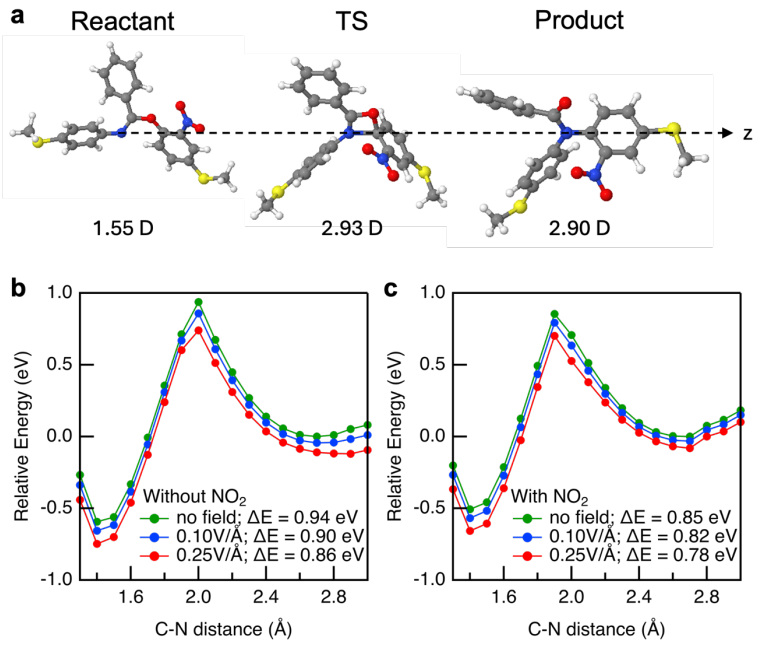

Figure 5. (a) DFT-optimized geometries of the Chapman species throughout the reaction. C and N atoms are constrained along the z-axis (dotted line), labeled with their respective dipole moments. DFT-calculated energies of reaction species (b) without and (c) with a nitro group, at different C-N bond distances without field (green), with 0.1 V/Å electric field (blue) and 0.25 V/Å electric field (red). Energy barriers between the reactant and transition state are indicated in the figure legend.

Conclusions and Future Outlooks

In conclusion, we have demonstrated that neither the Menshutkin reaction nor the Chapman rearrangement is accelerated in an electric field in the STM-BJ setup. We apply voltage biases within an STM-BJ setup to both generate a large local electric field and monitor reaction progress *in situ*, as well as HPLC and UPLC-MS analyses to track reaction progress *ex situ*. Previous theoretical studies have highlighted the importance of field orientation in electric-field-driven catalysis, and our findings support this. Although the Menshutkin reaction is predicted to be catalyzed by an electric field, only minor degrees of catalysis are expected when the reaction axis is not perfectly aligned with the external electric field[28]. Since our reactants are dissolved in solvent and are allowed to orient in the electric field, it is likely that there is imperfect alignment of the reaction axis with the external electric field. Furthermore, our studies suggest that in a system where the reaction axis is already pre-oriented in an intramolecular reaction (i.e., the Chapman rearrangement), the change in the reaction energy barrier with field is critical to determining whether an experimentally accessible electric field will catalyze the reaction. While we believe it is much more straightforward for theory to predict bond-breaking and isomerization reactions, care should be taken when using theory to predict bond-forming reactions. This is because in bond formation, the solvent, reactant dipoles, reaction axis, and field strength all affect the ability for the bond to form. These findings provide new insights into the field of electric-field-driven catalysis, and help outline a new set of empirically-confirmed guidelines for studying new reactions in electric fields.

Authors

Miriam Aziz – Department of Chemistry, Columbia University, New York, New York 10027, United States; orcid.org/0000-0002-8718-7220; Email: ma4110@columbia.edu

Claudia R. Prindle – Department of Chemistry, Columbia University, New York, New York 10027, United States; orcid.org/0009-0008-4111-3550; Email: crp2163@columbia.edu

Woojung Lee – Department of Chemistry, Columbia University, New York, New York 10027, United States; orcid.org/0000-0002-0384-5493; Email: wl2774@columbia.edu

Boyuan Zhang – Department of Chemistry, Fairfield University, Fairfield, Connecticut 06824, United States; orcid.org/0000-0001-8660-5796; Email: bzhang@fairfield.edu

Cedric Schaack –Department of Chemistry, Wake Forest University, Winston-Salem, North Carolina 27109, United States; orcid.org/0000-0003-4768-3374; Email: schaacc@wfu.edu

Fereshteh Zandkarimi – Department of Chemistry, Mass Spectrometry Core Facility, Columbia University, New York, New York 10027, United States; orcid.org/0000-0002-1120-3191; Email: fz2262@columbia.edu

Michael L. Steigerwald – Department of Chemistry, Columbia University, New York, New York 10027, United States; orcid.org/0000-0001-6337-2707; Email: mls2064@columbia.edu

ACKNOWLEDGMENT

This work was supported primarily by the NSF CHE-2023568 CCI Phase I: Center for Chemistry with Electric Fields. C.R.P. was supported by a National Defense Science and Engineering Graduate Fellowship. High resolution mass spectra (HR-MS) and liquid chromatograph mass spectra (LCMS) were obtained from the Columbia University Chemistry Department Mass Spectrometry Facility. We thank Dr. Liang Li and Wanzhuo Shi for helpful discussions.

SUPPORTING INFORMATION. Synthesis and Characterization; Additional Experiments; NMR Spectra.

References

(1) Anastas, P.; Eghbali, N. Green Chemistry: Principles and Practice*, Chem. Soc. Rev.* **2010**, *39*, 301.

(2) Cho, J.-Y.; Tse, M. K.; Holmes, D.; Maleczka, R. E.; Smith, M. R. Remarkably Selective Iridium Catalysts for the Elaboration of Aromatic C-H Bonds*, Science* **2002**, *295*, 305.

(3) Dasari, M. A.; Kiatsimkul, P.-P.; Sutterlin, W. R.; Suppes, G. J. Low-pressure hydrogenolysis of glycerol to propylene glycol*, Applied Catalysis A: General* **2005**, *281*, 225.

(4) Chiu, C.-W.; Dasari, M. A.; Suppes, G. J.; Sutterlin, W. R. Dehydration of glycerol to acetol via catalytic reactive distillation*, AIChE Journal* **2006**, *52*, 3543.

(5) Skucas, E.; Ngai, M.-Y.; Komanduri, V.; Krische, M. J. Enantiomerically Enriched Allylic Alcohols and Allylic Amines via C–C Bond-Forming Hydrogenation: Asymmetric Carbonyl and Imine Vinylation*, Acc. Chem. Res.* **2007**, *40*, 1394.

(6) Sheldon, R. A. E factors, green chemistry and catalysis: an odyssey*, Chem. Commun.* **2008**, 3352.

(7) Beach, E. S.; Cui, Z.; Anastas, P. T. Green Chemistry: A design framework for sustainability*, Energ. Environ. Sci.* **2009**, *2*, 1038.

(8) Leitner, W. Supercritical Carbon Dioxide as a Green Reaction Medium for Catalysis*, Acc. Chem. Res.* **2002**, *35*, 746.

(9) Thomas, J. M.; Raja, R. The advantages and future potential of single-site heterogeneous catalysts*, Topics in catalysis* **2006**, *40*, 3.

(10) Shaik, S.; Mandal, D.; Ramanan, R. Oriented electric fields as future smart reagents in chemistry*, Nat. Chem.* **2016**, *8*, 1091.

(11) Susarrey-Arce, A. *et al.* A new ATR-IR microreactor to study electric field-driven processes*, Sensors and Actuators B: Chemical* **2015**, *220*, 13.

(12) Arabi, A. A.; Matta, C. F. Effects of external electric fields on double proton transfer kinetics in the formic acid dimer, *Phys. Chem. Chem. Phys.* **2011**, *13*, 13738.

(13) Cerón-Carrasco, J. P.; Cerezo, J.; Jacquemin, D. How DNA is damaged by external electric fields: selective mutation vs. random degradation, *Phys. Chem. Chem. Phys.* **2014**, *16*, 8243.

(14) Carbonell, E.; Duran, M.; Lledos, A.; Bertran, J. Catalysis of Friedel-Crafts reactions by electric fields, *J. Phys. Chem.* **1991**, *95*, 179.

(15) Zhou, Z.-J.; Li, X.-P.; Liu, Z.-B.; Li, Z.-R.; Huang, X.-R.; Sun, C.-C. Electric Field-Driven Acid−Base Chemistry: Proton Transfer from Acid (HCl) to Base (NH3/H2O), *J. Phys. Chem. A* **2011**, *115*, 1418.

(16) Gorin, C. F.; Beh, E. S.; Kanan, M. W. An Electric Field–Induced Change in the Selectivity of a Metal Oxide–Catalyzed Epoxide Rearrangement, *J. Am. Chem. Soc.* **2012**, *134*, 186.

(17) Gorin, C. F.; Beh, E. S.; Bui, Q. M.; Dick, G. R.; Kanan, M. W. Interfacial Electric Field Effects on a Carbene Reaction Catalyzed by Rh Porphyrins, *J. Am. Chem. Soc.* **2013**, *135*, 11257.

(18) Albrecht, F.; Fatayer, S.; Pozo, I.; Tavernelli, I.; Repp, J.; Peña, D.; Gross, L. Selectivity in single-molecule reactions by tip-induced redox chemistry, *Science* **2022**, *377*, 298.

(19) Lin, J.; Lv, Y.; Song, K.; Song, X.; Zang, H.; Du, P.; Zang, Y.; Zhu, D. Cleavage of non-polar C(sp2)–C(sp2) bonds in cycloparaphenylenes via electric field-catalyzed electrophilic aromatic substitution, *Nat. Commun.* **2023**, *14*, 293.

(20) Basuri, P.; Mukhopadhyay, S.; Reddy, K. S. S. V. P.; Unni, K.; Spoorthi, B. K.; Shantha Kumar, J.; Yamijala, S. S. R. K. C.; Pradeep, T. Spontaneous α-C−H Carboxylation of Ketones by Gaseous CO2 at the Air-water Interface of Aqueous Microdroplets, *Angew. Chem. Int. Ed.* **2024**, *63*, e202403229.

(21) Spoorthi, B. K.; Debnath, K.; Basuri, P.; Nagar, A.; Waghmare, U. V.; Pradeep, T. Spontaneous weathering of natural minerals in charged water microdroplets forms nanomaterials, *Science* **2024**, *384*, 1012.

(22) Chen, H.; Wang, R.; Chiba, T.; Foreman, K.; Bowen, K.; Zhang, X. Designer "Quasi-Benzyne": The Spontaneous Reduction of Ortho-Diiodotetrafluorobenzene on Water Microdroplets, *J. Am. Chem. Soc.* **2024**, *146*, 10979.

(23) Aragonès, A. C.; Haworth, N. L.; Darwish, N.; Ciampi, S.; Bloomfield, N. J.; Wallace, G. G.; Diez-Perez, I.; Coote, M. L. Electrostatic catalysis of a Diels–Alder reaction, *Nature* **2016**, *531*, 88.

(24) Huang, X. *et al.* Electric field–induced selective catalysis of single-molecule reaction, *Sci. Adv.* **2019**, *5*, eaaw3072.

(25) Zang, Y. *et al.* Directing isomerization reactions of cumulenes with electric fields, *Nat. Commun.* **2019**, *10*, 4482.

(26) Zhang, B.; Schaack, C.; Prindle, C. R.; Vo, E. A.; Aziz, M.; Steigerwald, M. L.; Berkelbach, T. C.; Nuckolls, C.; Venkataraman, L. Electric fields drive bond homolysis, *Chem. Sci.* **2023**, *14*, 1769.

(27) Dutta Dubey, K.; Stuyver, T.; Kalita, S.; Shaik, S. Solvent Organization and Rate Regulation of a Menshutkin Reaction by Oriented External Electric Fields are Revealed by Combined MD and QM/MM Calculations, *J. Am. Chem. Soc.* **2020**, *142*, 9955.

(28) Ramanan, R.; Danovich, D.; Mandal, D.; Shaik, S. Catalysis of Methyl Transfer Reactions by Oriented External Electric Fields: Are Gold–Thiolate Linkers Innocent?, *J. Am. Chem. Soc.* **2018**, *140*, 4354.

(29) Shaik, S.; de Visser, S. P.; Kumar, D. External Electric Field Will Control the Selectivity of Enzymatic-Like Bond Activations, *J. Am. Chem. Soc.* **2004**, *126*, 11746.

(30) Hirao, H.; Chen, H.; Carvajal, M. A.; Wang, Y.; Shaik, S. Effect of External Electric Fields on the C−H Bond Activation Reactivity of Nonheme Iron−Oxo Reagents, *J. Am. Chem. Soc.* **2008**, *130*, 3319.

(31) Lai, W.; Chen, H.; Cho, K.-B.; Shaik, S. External Electric Field Can Control the Catalytic Cycle of Cytochrome P450cam: A QM/MM Study, *J. Phys. Chem. Lett.* **2010**, *1*, 2082.

(32) Hoffmann, N. M.; Wang, X.; Berkelbach, T. C. Linear Free Energy Relationships in Electrostatic Catalysis, *ACS Catalysis* **2022**, *12*, 8237.

(33) Venkataraman, L.; Klare, J. E.; Nuckolls, C.; Hybertsen, M. S.; Steigerwald, M. L. Dependence of single-molecule junction conductance on molecular conformation, *Nature* **2006**, *442*, 904.

(34) Nagahara, L. A.; Thundat, T.; Lindsay, S. M. Preparation and characterization of STM tips for electrochemical studies, *Rev. Sci. Instrum.* **1989**, *60*, 3128.

(35) Blum, V.; Gehrke, R.; Hanke, F.; Havu, P.; Havu, V.; Ren, X.; Reuter, K.; Scheffler, M. Ab initio molecular simulations with numeric atom-centered orbitals, *Comp. Phys. Comm.* **2009**, *180*, 2175.

(36) Arnold, A.; Weigend, F.; Evers, F. Quantum chemistry calculations for molecules coupled to reservoirs: Formalism, implementation, and application to benzenedithiol, *J. Chem. Phys.* **2007**, *126*, 174101.

(37) Bagrets, A. Spin-polarized electron transport across metal–organic molecules: a density functional theory approach, *J. Chem. Theory Comp.* **2013**, *9*, 2801.

(38) Perdew, J. P.; Burke, K.; Ernzerhof, M. Generalized gradient approximation made simple, *Phys. Rev. Lett.* **1996**, *77*, 3865.

(39) Bochevarov, A. D. *et al.* Jaguar: A high-performance quantum chemistry software program with strengths in life and materials sciences, *Int. J. of Quant. Chem.* **2013**, *113*, 2110.

(40) Sola, M.; Lledos, A.; Duran, M.; Bertran, J.; Abboud, J. L. M. Analysis of solvent effects on the Menshutkin reaction, *J. Am. Chem. Soc.* **1991**, *113*, 2873.

(41) Turan, H. T.; Brickel, S.; Meuwly, M. Solvent Effects on the Menshutkin Reaction, *J. Phys. Chem. B* **2022**, *126*, 1951.

(42) Menschutkin, N. Beiträge zur Kenntnis der Affinitätskoeffizienten der Alkylhaloide und der organischen Amine, *Z. Phys. Chem.* **1890**, *5U*, 589.

(43) Menschutkin, N. Über die Affinitätskoeffizienten der Alkylhaloide und der Amine, *Z. Phys. Chem.* **1890**, *6U*, 41.

(44) Castejon, H.; Wiberg, K. B. Solvent Effects on Methyl Transfer Reactions. 1. The Menshutkin Reaction, *J. Am. Chem. Soc.* **1999**, *121*, 2139.

(45) Chapman, A. W. CCXXVII.—Imino-aryl ethers. Part V. The effect of substitution on the velocity of molecular rearrangement, *J. Chem. Soc.* **1927**, *0*, 1743.

(46) Relles, H. M. Steric rate enhancement in the Chapman rearrangement, *J. Org. Chem.* **1968**, *33*, 2245.

Table of Contents Figure